Response variation of optically stimulated luminescence dosimeters

A. Asena [a,*], S.B. Crowe [a], T. Kairn [a,c], L. Dunn [d], M. Cyster [b], I.M. Williams [d], P.H. Charles [a], S.T. Smith [a], J.V. Trapp [a]

[a] School of Chemistry, Physics and Mechanical Engineering, Queensland University of Technology, Brisbane, QLD 4001, Australia
[b] School of Applied Science, Engineering and Health, RMIT, Melbourne VIC 3001, Australia
[c] Premion, The Wesley Medical Centre, Suite 1, 40 Chasely St, Auchenflower, QLD 4066, Australia
[d] Australian Radiation Protection and Nuclear Safety Agency, 619 Lower Plenty Road, Yallambie VIC, 3085, Australia
* Corresponding author. E-mail address: a.asena@qut.edu.au

A B S T R A C T

This study investigates the variability in response of optically stimulated luminescence dosimeters (OSLDs). Examining the source of sensitivity variations in these dosimeters allows for a more comprehensive understanding of the Landauer nanoDots and their potential for current and future applications. In this work, OSLDs were scanned with a MicroCT scanner to determine potential sources for the variation in relative sensitivity across a selection of Landauer nanoDot dosimeters. Specifically, the correlation between a dosimeters relative sensitivity and the loading density of Al_2O_3:C powder was determined. When extrapolating the sensitive volume's radiodensity from the CT data, it was shown that there is a non-uniform distribution in crystal growth. It was calculated that a 0.05% change in the nominal volume of the chip produces a 1% change in the overall response. Additionally, the 'true' volume of an OSLD's sensitive material is, on average, 18% less than that which has been reported in literature, mainly due to the presence of air cavities in the material's structure. This work demonstrated that the amount of sensitive material is approximately linked to the total correction factor.

Key words: optically stimulated luminescence dosimeter, micro computed tomography, element correction factor, response and sensitivity.

1. Introduction

The success of curative intended radiation therapy is largely dependent on the ability to deliver the prescribed radiation dose to the patient within a narrow tolerance. Dosimeters can be placed in anthropomorphic phantoms to verify the delivered dose. In the past, these studies have employed the use of thermoluminescent dosimeters (TLDs), because their small size makes them practical for this purpose (Ertl et al., 1997). Optically stimulated luminescent dosimeters (OSLDs) are now being employed as a replacement because of their faster processing times and simple readout procedures (McKeever et al., 2003). Dunn et al. (2013) has presented a series of characterisations of the Landauer nanoDot OSLDs that include batch characteristics, post-readout signal depletion, signal stability, linearity of dose response, energy dependence and bleaching for re-use. Jursinic et al. (2007) and Yukihara et al. (2004) have reported similar results.

Optically stimulated luminescence (OSL) uses the ability of materials like Al_2O_3:C to store absorbed dose and then release it as light upon stimulation. The crystal imperfections act as traps for electrons and vary in depth since there is a spectrum of stimulation allowable, and trap levels responsible, for the OSL. The sensitivity of the material is related to the density of recombination centres (McKeever et al., 1999), which is in the range of 10^{15}-10^{16} cm^{-3}. Because of this non-uniform distribution of traps in crystal growth the sensitivity varies substantially within a batch of dosimeters.

While it is easy to correct for this variation in sensitivity using individual element correction factors (ECFs) (Dunn et al., 2013), a quantitative understanding of the relationship between ECF and sensitive volume has not yet been investigated or reported in literature. We hypothesize that the source of the varying element correction factor is directly linked to the sensitive volume contained within the OSLD. An in-depth 3D exploration of the luminescent dosimeter's sensitive material can be achieved via micro computed tomography (MicroCT). We present an evaluation of a possible cause for the observed changes in the sensitivity of nanoDots, which is accomplished by examining the response of select nanoDots with differing sensitive volumes.

2. Materials and Methods

The dosimeters used in this study were nanoDot OSLDs (Landauer Inc., Glenwood, IL). The dosimeter material is housed in a plastic light-tight casing, measuring 10×10×2 mm^3. The detector is a composite printed layer of Al_2O_3 powder and polyester binder (0.15 mm) on polyester substrate (0.15 mm) with cover tape (0.05 mm) used for binding, putting the total disk thickness near 0.35 mm (Perks et al., 2008).

Irradiations were performed with an Eldorado (Model G) Co-60 teletherapy unit (Atomic Energy of Canada Ltd, Chalk River, Canada).

In order to account for the individual sensitivities of different dosimeters, a group of nanoDots was irradiated with a 1 Gy dose. The mean signal of the batch was calculated and an ECF determined for each dosimeter (Dunn et al., 2013). The response of individual dosimeters was compared to the average of the group reading and from the ratio a correction factor was determined.

A selection of 11 Landauer nanoDot OSLDs with ECFs varying from 0.94-1.05 were scanned in a Scanco Medical µCT 40 Cone-Beam Micro Computed Tomography Scanner (SCANCO Medical AG, Basserdorf, Switzerland) with a nominal x-ray energy of 55kVp and a tube current of 145µA. After being scanned as a single stack, a series of TIFF and DICOM images were generated. The scanner has an isotropic resolution of 20 microns with a maximum field of view of 1024×1024. For each dosimeter, 36 image slices were used in the analysis.

The MicroCT data was imported into MATLAB (version 7.10.0.499, The MathWorks). The TIFF and DICOM data sets allowed two distinct approaches for analysis given their differing bit depths. The first analysis utilised the data in TIFF format, allowing the relative volume of each OSLD to be calculated. A square region of interest (ROI) was defined, each consisting of 380x380 pixels centred on the location of the Al_2O_3:C chip. This greyscale image was converted to a binary image based on a choice of pixel threshold, i.e. matrix elements equal to, or above the threshold were given a value of 1 (white pixel), while those matrix elements below, were replaced by a 0 (black pixel). Subsequently, an iterative loop allowed the number of white pixels across each individual OSLD to be counted. The choice of a pixel threshold involved generating a histogram to display the number of voxels accumulated for each grayscale value as illustrated in Fig 1(a). From this analysis, two distinct peaks were observed; one relating to the sensitive material, and the other to the binding film. It was this observation that informed the threshold choice of 0.15 (relating to a grayscale value of 38).

The DICOM data was used to determine the radiodensity, or radiolucency, of relevant voxels. Again, a rectangular ROI centered on the location of the Al_2O_3:C chip was defined, each consisting of 380x380 pixels. From a series of 396 processed DICOM images, the Hounsfield unit (HU) for each pixel was acquired by means of a linear transformation. Image slices of each OSLD consisting of 2500 pixels were averaged to determine HU of Al_2O_3:C. The standard deviation was calculated for these specified regions to provide approximate errors and roughly indicate the variation in voxel radiodensity. Following this, the number of voxels above specified radiodensities threshold was counted for each of the eleven nanoDots. Thresholds were imposed to minimize the accumulation of false artefacts, and the selections were informed by generating a histogram, shown in Fig 1(b), to display the number of voxels accumulated for each Hounsfield Unit. From this, two peaks were observed relating to the binding film and sensitive material; however, the peak separation was less discernible and thus a number of different thresholds (1000HU, 1500HU and 2000HU) were examined to determine which would be more statistically significant.

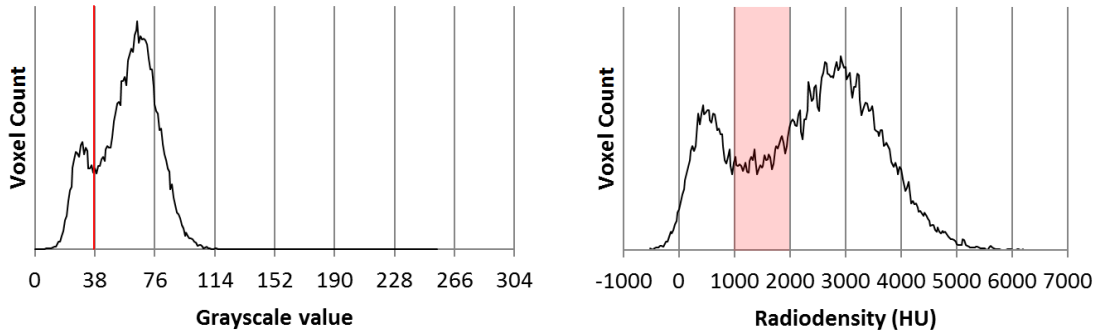

Figure 1. Histograms generated for OSLDs from both the TIFF (a) and DICOM (b) data sets, showing the voxel count vs. grayscale value (TIFF) and the voxel count vs. radiodensity (DICOM).

Obtaining the average radiodensity for a single OSLD was achieved via similar methods. To minimize the averaging of false artefacts, a threshold was once again imposed. A cutoff of 1500HU would allow for the Al_2O_3:C voxels to be averaged, while ignoring the surrounding or internal air cavities and polyester film.

3. Results and Discussion

Figs 2(a) and (b) show multiple 20μm resolution scans for five different dosimeters. Fig 2(a) illustrates the recurring presence of internal air cavities. Furthermore, the method employed to extrapolate the volume was influenced by small errors as shown by the regular presence of outlier pixels demonstrated in Fig 2(b).

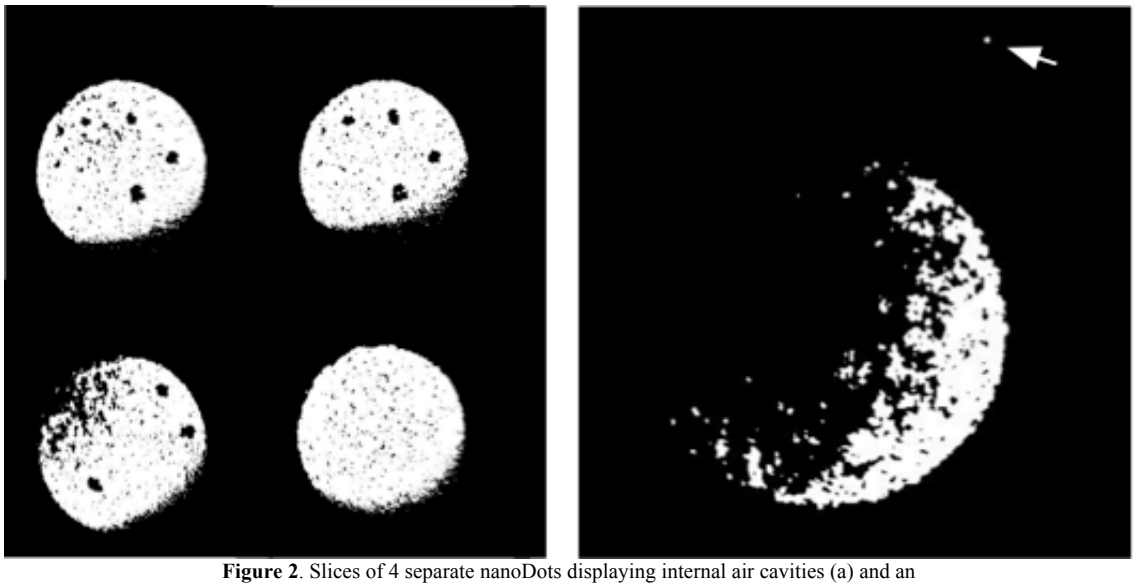

Figure 2. Slices of 4 separate nanoDots displaying internal air cavities (a) and an example of how outlier pixels erroneously contribute to the voxel count (b).

Examining the source of sensitivity variations in Al_2O_3:C allows for a more comprehensive understanding of the Landauer nanoDots and their potential for current and future applications. The MicroCT scanner produced isotropic voxels with equal dimensions in x, y and z orientation. Given the scanner's spatial resolution, and the published dimensions of the sensitive material, the expected number of voxels for the method of binary conversion was calculated to be approximately $3.67\times10^5 \pm 10\%$. However, the average white voxel count accumulated, on average, was 82% of this figure. This would suggest that the 'true' volume of an OSLD's sensitive material is, on average, 18% less than that which has been reported in literature (Charles et al., 2012), mainly due to the presence of air cavities in the material's structure. This difference is important, for example, when developing Monte Carlo models of the dosimeters for radiotherapy applications, where a precise understanding of the sensitive material's volume is important.

Fig. 3 shows a plot of voxel count versus the element-specific correction factor derived from a series of 396 TIFF images, where each point represents a single OSLD. A line was fitted which has an R^2-value of 0.69 and a P-value of 1.56×10^{-3}. This data shows that the response of a dosimeter decreases proportionally with sensitive volume.

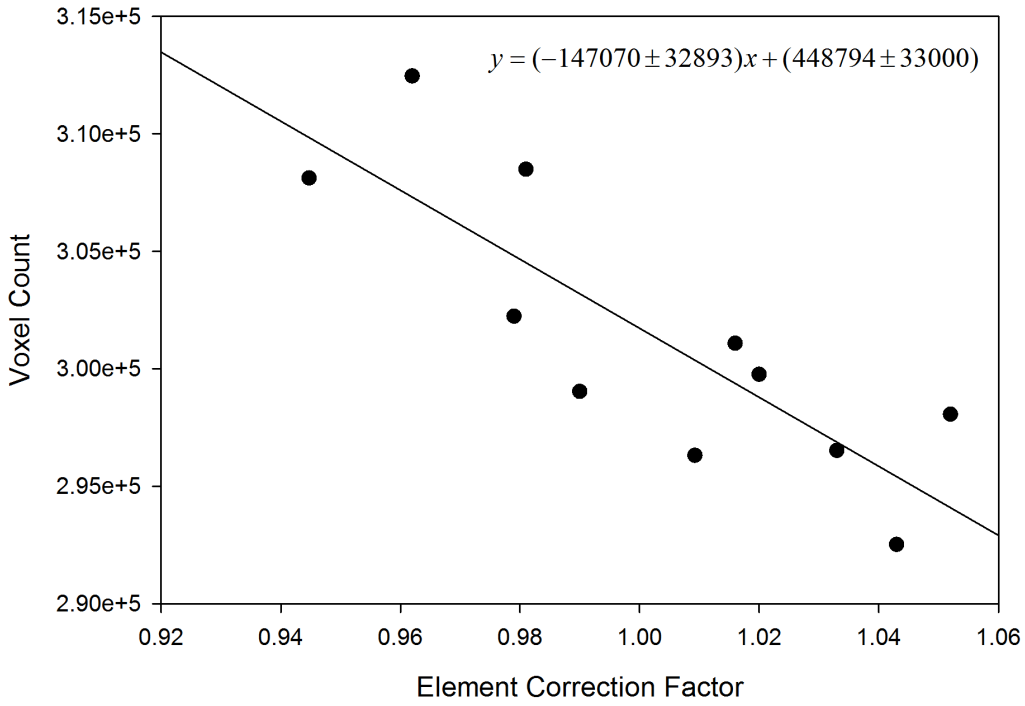

Figure 3. Eleven nanoDot's sensitive volume plotted against their individual element correction factors.

By extrapolating from Fig. 3, a quantitative relationship between response and sensitive volume can be roughly determined for this batch of dosimeters. A change in volume of 1.176×10^{-5} cm^3 corresponds to a 1% change in response. In other words, a 0.05% change in the nominal volume of the chip would result in a 1% change in response. The observed increase in pixel counts doesn't correspond to a perfectly linear increase in response because the active ingredient concentration may not consistently or monotonically increase with chip volume, for chips this small. Furthermore, the potential effects of the inaccuracy of Al_2O_3:C deposition increases with decreasing chip size. If a luminescent dosimeter were manufactured with a smaller volume than currently employed using the same manufacturing protocol, the variation in response from chip to chip would more than likely exceed the current 5% range.

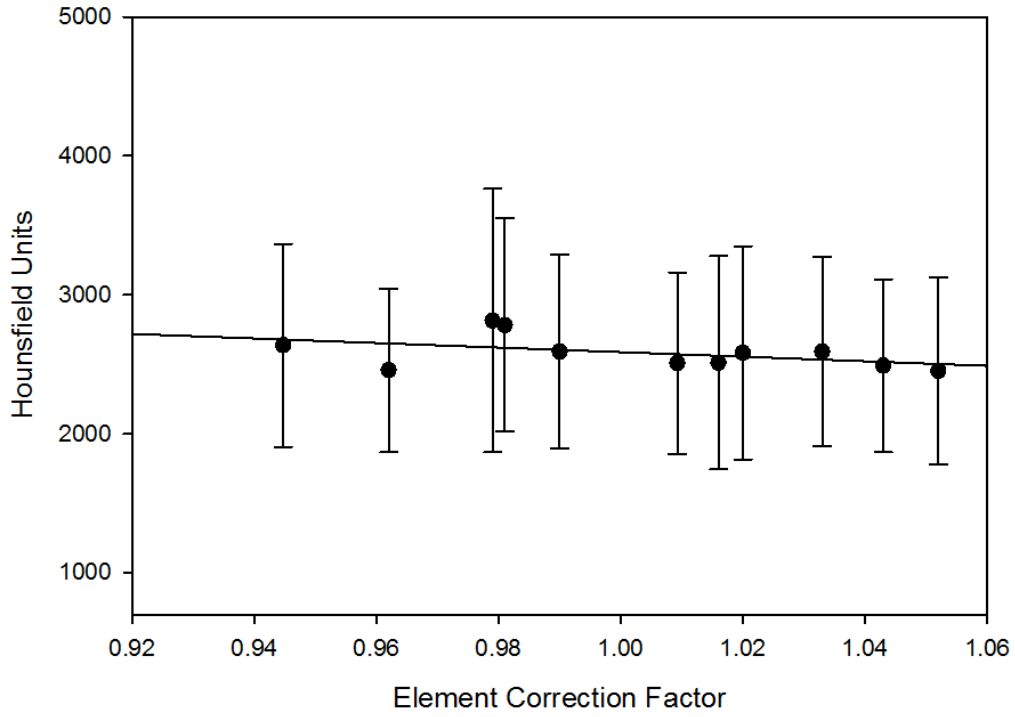

Figure 4. Average radiodensity of voxels above 1500HU for the eleven tested Landauer nanoDots.

The initial analysis showed Al_2O_3:C to have an average radiodensity of 3000±800 HU. Fig. 4 shows the average radiodensity of the eleven Landauer nanoDots for values above a selected CT number. Each point corresponds to one of the eleven dosimeters used. The threshold was chosen based on the prior analysis of aluminum oxide's range of radiodensities. A trendline was fit to the data that had an R^2-value of 0.22 and a P-value of 0.15. Fig. 4 shows a negligible correlation between average HU and individual sensitivity.

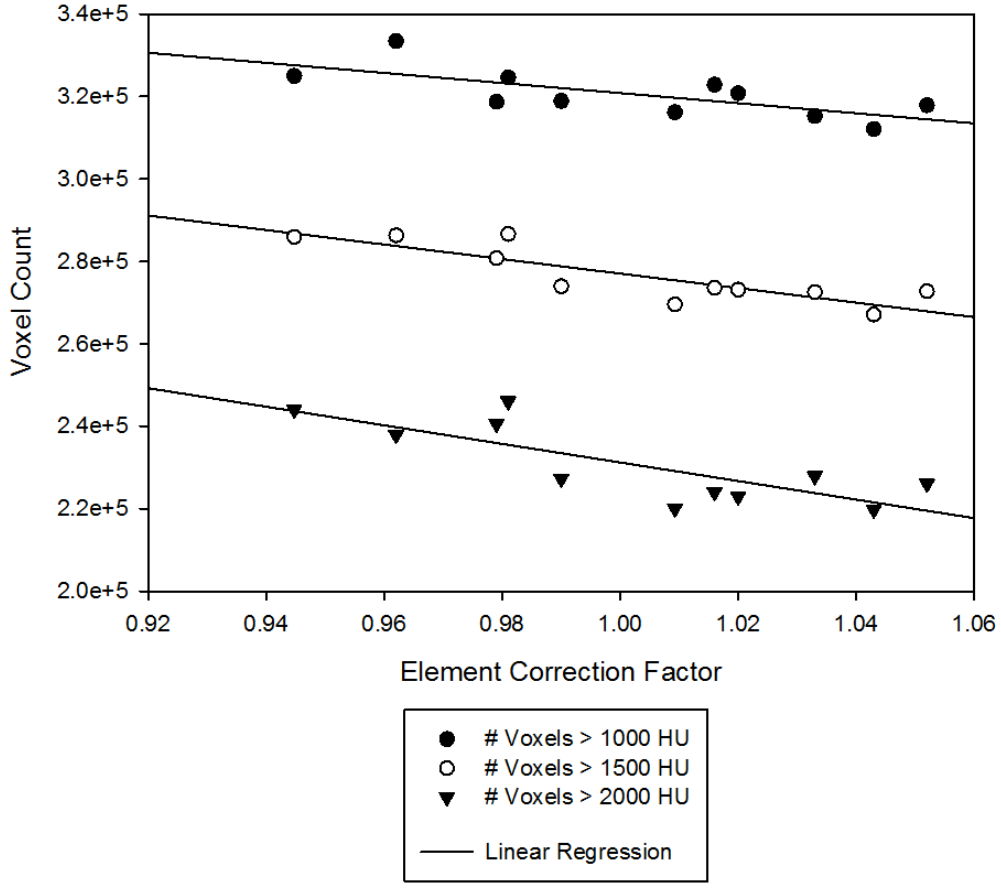

Figure 5. Relative sensitive volumes of eleven OSLDs based on accumulation of voxels above thresholds of 1000, 1500 and 2000HU.

Fig. 5 shows a plot of the voxel count in an OSLD's sensitive material, which have values above a selected radiodensity. Each point corresponds to one of the eleven dosimeters used. The thresholds were chosen based on the prior analysis of aluminum oxide's range of radiodensities. R^2 and P-values were determined for each set of data with the strongest statistical significance and linearity ($P = 0.001$, $R^2 = 0.73$) arising from a HU cutoff of 1500HU compared to 1000HU ($P = 0.013$, $R^2 = 0.52$) and 2000HU ($P = 0.004$, $R^2 = 0.63$). This figure demonstrates the relationship between the dosimeter's radiodensity, sensitive volume, and response as well as identifying an accurate radiodensity threshold for the OSLDs. The voxels with radiodensities around 1000HU would be susceptible to false averaging with surrounding air cavities or binding film. This is a factor that is less prominent for a 1500HU cut-off, thus we see results with a higher statistical significance.

4. Conclusions

This work has shown that the amount of sensitive material is linked to the total correction factor. However, this increase in volume did not correspond to a perfectly linear increase in response. This would suggest that a small change in volume is not proportional to the change in the number of luminescent centres due to the heterogeneity of Al_2O_3 deposition. An average radiodensity of 3000±800 HU was calculated for the dosimeters sensitive material. The study showed that a 0.05% change in the nominal volume of the chip corresponds to a 1% change in response. Furthermore, the 'true' volume of an OSLD's sensitive material is, on average, 18% less than that which has been reported in literature, mainly due to the presence of air cavities in the material's structure.

Acknowledgments

This study was supported by the Australian Research Council, the Wesley Research Institute, Premion and the Queensland University of Technology (QUT), through linkage grant number LP110100401. The authors would like to formally acknowledge ARPANSA for use of the primary standard Co-60 facility located at ARPANSA and the Australian Clinical Dosimetry Service, a joint initiative between the Department of Health and the Australian Radiation Protection and Nuclear Safety Agency.

REFERENCES

Charles, P.H., Crowe, S.B., Kairn, T., Kenny, J., Lehmann, J., Lye, J., Dunn, L., Hill, B., Knight, R.T., Langton, C.M., Trapp, J.V., 2012. The effect of very small air gaps on small field dosimetry. Phys. Med. Biol. 57 (21), 6947-6960.

Dunn, L., Lye, J., Kenny, J., Lehmann, J., Williams, I., and Kron, T., 2013. Commissioning of optically stimulated luminescence dosimeters for use in radiotherapy. Rad. Meas., 51, 31-39.

Ertl, A., Zehetmayer, M., Schaggl, A., Kindl, P., and Hartl, R., 1997. Dosimetry studies with TLDs for stereotactic radiation techniques for intraocular tumours. Phys. Med. Biol. 42 (11), 2137-2145.

Jursinic, P.A., 2007. Characterization of optically stimulated luminescent dosimeters, OSLDs, for clinical dosimetric measurements. Med. Phys. 34, 4594–4604.

McKeever, S.W.S., Moscovitch, M., 2003. On the advantages and disadvantages of optically stimulated luminescence dosimetry and thermoluminescence dosimetry. Rad. Protec. Dos. 104 (3), 263–270.

Perks, C.A., Yahnke, C., Million, M., 2008. Medical dosimetry using Optically Stimulated Luminescence dots and microStar readers. In 12th International Congress of the International Radiation Protection Association.

Yukihara, E.G., Whitley, V.H., McKeever, S.W.S., Akselrod, A.E., Akselrod, M.S., 2004. Effect of high-dose irradiation on the optically stimulated luminescence of Al_2O_3:C. Rad. Meas. 38 (3), 317–330.